Hyperfine Interact
DOI 10.1007/s10751-013-0930-6

Local structure and water cleaning ability of iron oxide nanoparticles prepared by hydro-thermal reaction

Koya Shibano · Shiro Kubuki · Kazuhiko Akiyama · Zoltán Homonnay · Ernő Kuzmann · Stjepko Krehula · Mira Ristić · Tetsuaki Nishida

Abstract Nanoparticles (NPs) of Fe_3O_4 and γFe_2O_3 synthesized by hydrothermal reaction were characterized by X-ray diffractometry (XRD), ^{57}Fe-Mössbauer spectroscopy and field emission scanning electron microscopy (FE-SEM). A decrease in concentration of methylene blue (MB) aqueous solution due to bulk Fe^0-NP γFe_2O_3 mixture with the mass ratio of 3:7 was measured by ultraviolet-visible light absorption spectroscopy (UV-Vis). The Mössbauer spectrum of NP Fe_3O_4 prepared from hydrothermal reaction was composed of two sextets with absorption area (A), isomer shift (δ) and internal magnetic field ($H_{\rm int}$) of 56.3 %, $0.34_{\pm 0.03}$ mm s^{-1} and $49.0_{\pm 0.30}$ T for tetrahedral ($T_{\rm d}$) Fe^{III}, and 43.7 %, $0.66_{\pm 0.11}$ mm s^{-1} and $44.0_{\pm 0.71}$ T for octahedral ($O_{\rm h}$) Fe^{II+III}. The Fe^{II}/Fe^{III} ratio was determined to be 0.280 for NP Fe_3O_4, giving 'x' of 0.124 in $Fe_{3-x}O_4$. These results show that NP Fe_3O_4 prepared by hydrothermal reaction was not regular but nonstoichiometric Fe_3O_4. Consistent

Proceedings of the 32nd International Conference on the Applications of the Mössbauer Effect (ICAME 2013) held in Opatija, Croatia, 1–6 September 2013.

K. Shibano · S. Kubuki (✉) · K. Akiyama
Department of Chemistry, Graduate School of Science and Engineering,
Tokyo Metropolitan University, Minami-Osawa 1-1, Hachi-Oji, Tokyo 192-0397, Japan
e-mail: kubuki@tmu.ac.jp

Z. Homonnay · E. Kuzmann
Laboratory of Nuclear Chemistry, Institute of Chemistry, Eötvös Loránd University,
Pázmany P. s., 1/A, Budapest 1117, Hungary

S. Krehula · M. Ristić
Division of Materials Chemistry, Ruđer Bošković Institute,
P. O. Box 180, Zagreb 10002, Croatia

T. Nishida
Department of Biological and Environmental Chemistry,
Faculty of Humanity-Oriented Science and Engineering,
Kinki University, Kayanomori 11-6, Iizuka, Fukuoka 820-8555, Japan

Published online: 30 October 2013

results were observed for XRD patterns of NP $Fe_{3-x}O_4$ indicating sharp intense peaks at 2Θ of 30.2, 35.7 and 43.3° with a large linewidth of 0.44°, yielding the crystallite size of 29–37 nm from the Scherrer's equation. Iso-thermal annealing of NP $Fe_{3-x}O_4$ at 250 °C for 30 min resulted in the precipitation of NP γFe_2O_3 with δ of $0.33_{\pm 0.03}$ mm s^{-1} and H_{int} of $46.4_{\pm 0.27}$ T due to magnetic tetrahedral Fe^{III}. The Debye temperature of NP $Fe_{3-x}O_4$ was respectively estimated to be $267_{\pm 5.45}$ K for $Fe^{III}(T_d)$ and $282_{\pm 7.17}$ K for $Fe^{II+III}(O_h)$, both of which were smaller than that obtained for bulk Fe_3O_4 of $280_{\pm 4.15}$ K and $307_{\pm 5.70}$ K, indicating that the chemical environment of iron of NPs is less rigid than that of the bulk compounds. A leaching test using methylene blue (MB) and mixture of bulk Fe^0-NP γFe_2O_3(3:7) showed a remarkable decrease in MB concentration from $1.90 \times 10^{-2}$to 9.49×10^{-4} mM for 24 h with the first order rate constant (k_{MB}) of 2.1×10^{-3} min^{-1}. This result verifies that MB decomposing ability is enhanced by using NP γFe_2O_3 compared with the k_{MB} of 1.1×10^{-4} min^{-1} previously obtained from the leaching test using MB and bulk mixture of $Fe^0 - \gamma Fe_2O_3$ (3:7).

Keywords Nano particle · Maghemite · Magnetite · Methylene blue · ^{57}Fe-Mössbauer spectroscopy · Debye temperature

1 Introduction

Ferrite nanoparticles attract much interest because they are applicable for environmental purification. For example, V-Ti co-doped magnetite decomposed methylene blue (MB) with the first order rate constant of 1.34 min^{-1} by Fenton reaction [1]. On the other hand, Pathak et al. revealed that $Mg_xMn_{(1-x)}Fe_2O_4$ decomposed nitrobenzene in water by the photocatalytic effect [2]. However, there are several difficulties in quantitative evaluation of both the Fenton reaction and the photo-catalytic reaction. Our previous studies revealed that an industrially-produced Fe^0-γFe_2O_3 mixture decreased the concentration of trichloroethylene (TCE) in aqueous solution from 10 to 0.5 mg L^{-1} after 7-day leaching [3]. Decomposition of organic compounds by applying an Fe^0-γFe_2O_3 mixture is superior to that of Fenton reaction and photo-catalytic reaction because the condition control is quite simple. It can be expected that toxic organic compounds like TCE could be decomposed more effectively by Fe^0-γFe_2O_3 mixture of smaller particle size. In this study, nanoparticles (NPs) of Fe_3O_4 and γFe_2O_3 were prepared by hydrothermal reaction, and the structure and methylene blue decomposing ability were investigated by ^{57}Fe-Mössbaur spectroscopy, X-ray diffractometry (XRD) and ultraviolet-visible light absorption spectroscopy (UV-Vis).

2 Experimental

Nanoparticles (NPs) of Fe_3O_4 and γFe_2O_3 were prepared by hydrothermal reaction. $(NH_4)_2Fe(SO_4)\cdot 6H_2O$ (Mohr salt) with the weight of 1.960 g was dissolved in 7 mL of deionized water. Separately, 2.702 g of $FeCl_3\cdot 6H_2O$ was dissolved in 32 mL of absolute ethanol. Solutions of Mohr salt and $FeCl_3$were mixed by a magnetic stirrer.

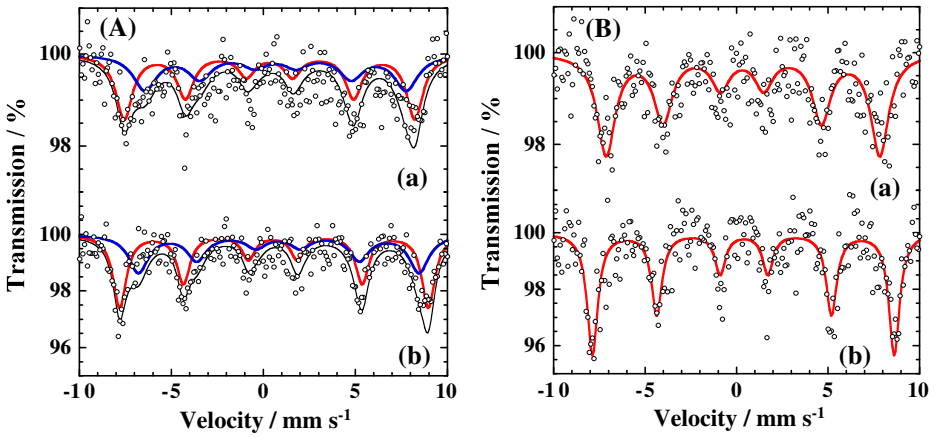

Fig. 1 Mössbauer spectra of NPs of (**A**) $Fe_{3-x}O_4$ and (**B**) γ-Fe_2O_3 measured at (**a**) 300 K and (**b**) 77 K

A black precipitate appeared when 10 mL of 25vol. % NH_3aqueous solution was added in droplets. The resulting solution including black precipitate was transferred to an autoclave and hydrothermally treated at 140 °C for 2 h. The black precipitate was separated from the mother liquor by centrifuging under 9000 r.p.m. for 5 min. NP $Fe_3O_4$was obtained by overnight drying of the black precipitate which was collected after washing several times by distilled water and ethanol. NP γFe_2O_3 was prepared by annealing of the synthesized NP Fe_3O_4 at 250 °C in air for 30 min.

The structural characterization of NPs of $Fe_3O_4$and $\gamma Fe_2O_3$was carried out by ^{57}Fe-Mössbauer spectroscopy, X-ray diffractometry (XRD) and a field emission scanning electron microscopy (FE-SEM). Mössbauer spectra were measured between 77 and 300 K by a constant acceleration method with a source of ^{57}Co(Rh) and with α-Fe as a reference. XRD measurements were conducted in the 2θ from 10 to 80° at 0.02° intervals with a scanning rate of 5°min^{-1}, using Cu-K_α (λ = 0.1541 nm) radiation emitted under the tube voltage and current of 50 kV and 300 mA, respectively. FE-SEM observation was carried out with the magnification of up to 3.3×10^4 by setting the voltage at 5.0 kV. The samples were not coated with an electrically conductive layer. The purity of each NP was checked using the energy dispersive X-ray analyzer under the voltage of 10 kV and the current of 3.0×10^{-9} A. A leaching test was performed with 2.0×10^{-2} mM of 20 mL methylene blue (MB) aqueous solution and 100 mg of bulk Fe^0-NP γFe_2O_3 mixture for 24 h. UV-Vis spectra were measured in the wavelength range of 200 and 800 nm, using a source of tungsten-deuterium lamp under an output power of 20 W.

3 Results and discussion

Mössbauer spectra of NPs of Fe_3O_4 and γFe_2O_3measured at 300 K and 77 K are shown in Fig. 1, the corresponding Mössbauer parameters are listed together with those of bulk Fe_3O_4 and γFe_2O_3 in Table 1. The Mössbauer spectrum of NP Fe_3O_4 measured at 300 K is composed of two magnetic sextets with respective isomer shift

Table 1 Temperature dependence of ^{57}Fe-Mössbauer parameters of nano and bulk particles of Fe_3O_4 and γFe_2O_3

		T (K) species	77	100	150	200	250	300
			Isomer shift : δ (mm s^{-1})					
Fe_3O_4	NP	$Fe^{III}(T_d)$	0.53	0.52	0.45	0.42	0.39	0.34
		$Fe^{II+III}(O_h)$	0.74	0.70	0.71	0.69	0.68	0.66
	Bulk	$Fe^{III}(T_d)$	0.51	0.50	0.46	0.41	0.34	0.32
		$Fe^{II+III}(O_h)$	0.81	0.77	0.76	0.71	0.66	0.65
γFe_2O_3	NP	$Fe^{III}(T_d)$	0.39	0.38	0.36	0.40	0.34	0.33
	Bulk	$Fe^{III}(T_d)$	0.48	0.48	0.46	0.43	0.40	0.37
			Internal magnetic field: H_{int} (T)					
Fe_3O_4	NP	$Fe^{III}(T_d)$	52.0	52.8	50.9	50.6	50.1	49.0
		$Fe^{II+III}(O_h)$	47.3	47.7	45.3	46.3	44.1	44.0
	Bulk	$Fe^{III}(T_d)$	51.4	51.4	51.0	50.4	50.0	49.2
		$Fe^{II+III}(O_h)$	47.3	47.6	47.3	46.7	46.3	45.5
γFe_2O_3	NP	$Fe^{III}(T_d)$	51.2	50.8	50.3	51.0	47.3	46.4
	Bulk	$Fe^{III}(T_d)$	52.5	52.3	52.0	51.5	50.7	49.9
			FWHM : Γ (mm s^{-1})					
Fe_3O_4	NP	$Fe^{III}(T_d)$	0.87	0.82	0.68	0.65	0.87	1.09
		$Fe^{II+III}(O_h)$	1.29	0.92	0.91	1.16	1.26	1.55
	Bulk	$Fe^{III}(T_d)$	0.66	0.60	0.52	0.49	0.47	0.46
		$Fe^{II+III}(O_h)$	0.66	0.60	0.52	0.49	0.47	0.46
γFe_2O_3	NP	$Fe^{III}(T_d)$	0.85	0.91	1.05	0.83	1.10	1.21
	Bulk	$Fe^{III}(T_d)$	0.57	0.57	0.55	0.54	0.54	0.55
			Absorption area : A (%)					
Fe_3O_4	NP	$Fe^{III}(T_d)$	54.8	54.9	52.6	59.2	54.9	56.3
		$Fe^{II+III}(O_h)$	45.2	45.1	47.4	40.8	45.1	43.7
	Bulk	$Fe^{III}(T_d)$	70.3	63.7	59.6	55.8	55.2	54.8
		$Fe^{II+III}(O_h)$	29.7	36.3	40.4	44.2	44.8	45.2
γFe_2O_3	NP	$Fe^{III}(T_d)$	100	100	100	100	100	100
	Bulk	$Fe^{III}(T_d)$	100	100	100	100	100	100

(δ), internal magnetic field (H_{int}) and linewidth (Γ) of $0.34_{\pm 0.03}$ mm s^{-1}, $49.0_{\pm 0.30}$ T and $1.09_{\pm 0.03}$ mm s^{-1} due to tetrahedral (T_d) Fe^{III}, and of $0.66_{\pm 0.11}$ mm s^{-1}, $44.0_{\pm 0.71}$ T and $1.55_{\pm 0.31}$ mm s^{-1} due to octahedral (O_h) Fe^{II+III}. The absorption area (A) of $Fe^{III}(T_d)$ and $Fe^{II+III}(O_h)$ was determined to be 56.3 and 43.7 %, which indicates that NP Fe_3O_4 prepared by hydrothermal reaction is not regular but defective Fe_3O_4 denoted as $Fe_{3-x}O_4$. The values of 'x' and Fe^{II}/Fe^{III} rate indicated as '$r(Fe^{II}/Fe^{III})$' in NP $Fe_{3-x}O_4$ can be calculated by the following equations [4];

$$x = (2 - A\left(Fe^{II+III}(O_h)\right)/A\left(Fe^{III}(T_d)\right)/\left(5 \times A\left(Fe^{II+III}(O_h)\right)/A\left(Fe^{III}(T_d)\right) + 6\right), \quad (1)$$

$$r\left(Fe^{II}Fe^{III}\right) = \left\{A\left(Fe^{II+III}(O_h)\right)2\right\}/\left\{A\left(Fe^{II+III}(O_h)\right)/2 + A\left(Fe^{III}(T_d)\right)\right\}. \quad (2)$$

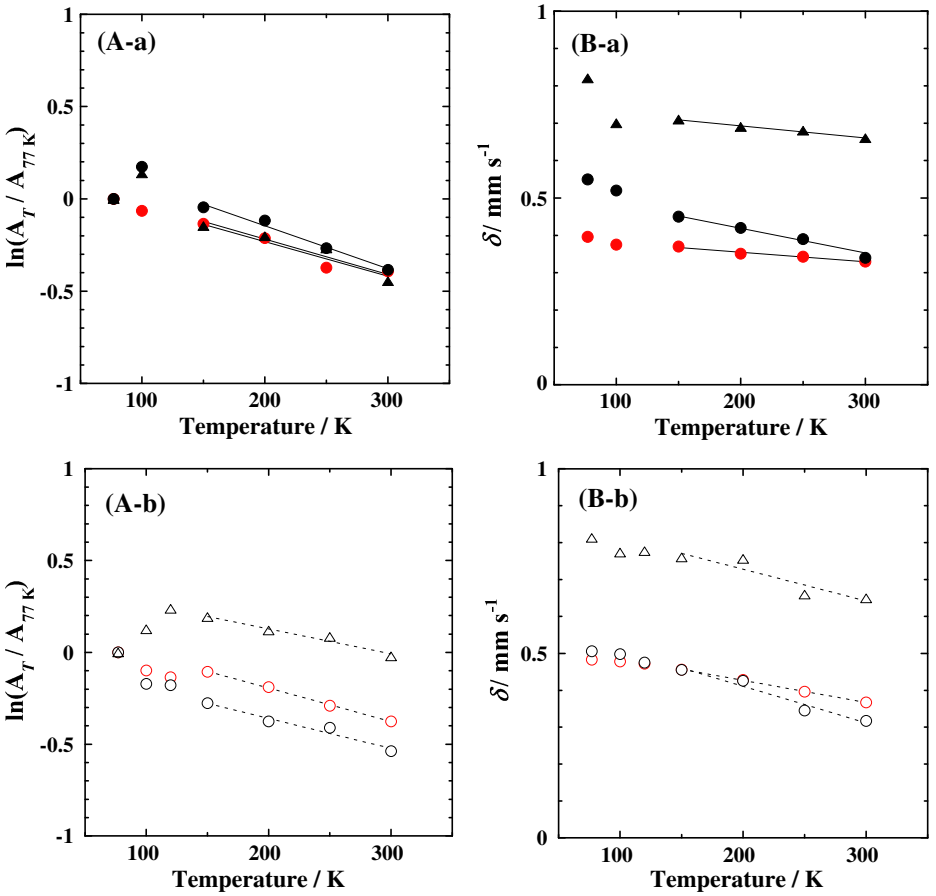

Fig. 2 Temperature dependences of (**A**) ln ($A_T/A_{77\,K}$) and (**B**) δ of (**a**) NPs and (**b**) bulk samples of Fe_3O_4 (*black*) and γ-Fe_2O_3 (*red*) attributed to tetrahedral Fe^{III} (*circle*) and octahedral Fe^{II+III} (*triangle*)

From A values of $Fe^{III}(T_d)$ (= 56.3 %) and that of Fe^{II+III} (O_h) (= 43.7 %) obtained from the Mössbauer spectrum of NP $Fe_{3-x}O_4$ measured at 300 K, the values of 'x' and $r(Fe^{II}/Fe^{III})$ were calculated to be 0.124 and 0.280, respectively. These results show that NP $Fe_{3-x}O_4$ prepared by the hydrothermal reaction is not regular but defective Fe_3O_4containing vacant $Fe^{II+III}(O_h)$ sites. δ values of $0.53_{\pm 0.02}$ and $0.74_{\pm 0.08}$ mm s^{-1} measured at 77 K (Fig. 1, (A-b)), respectively, attributed to tetrahedral (T_d) Fe^{III} and octahedral (O_h) Fe^{II+III} decreased to $0.34_{\pm 0.03}$ and $0.66_{\pm 0.11}$ mm s^{-1} at 300 K (Figs. 1 and 2 (A-a)). The Debye temperature (Θ_D) can be calculated from (3):

$$-\ln f = \left[-\frac{3E^2}{k\Theta_D Mc^2} \left(\frac{1}{4} + \left(\frac{T}{\Theta_D} \right)^2 \int_0^{\Theta_D/T} \frac{x dx}{(e^x - 1)} \right) \right], \tag{3}$$

Table 2 The Debye temperature of nano and bulk particles of Fe_3O_4 and γFe_2O_3derived from (4) (Θ_D)and from (7) (Θ_D')

		Species	$d\ln[A_T/A_{77\,K}]/dT$	Θ_D(K)	Θ_D'(K)
Fe_3O_4	NP	$Fe^{III}(T_d)$	-2.33×10^{-3}	264	267
		$Fe^{II+III}(O_h)$	-1.92×10^{-3}	270	282
	Bulk	$Fe^{III}(T_d)$	-1.36×10^{-3}	265	280
		$Fe^{II+III}(O_h)$	-1.64×10^{-3}	304	307
γFe_2O_3	NP	$Fe^{III}(T_d)$	-1.36×10^{-3}	256	259
	Bulk	$Fe^{III}(T_d)$	-1.87×10^{-3}	287	265

where f, k, M and c are recoil free fraction, Boltzmann constant, mass of the Mössbauer nuclei, and speed of light in vacuum [5, 6]. For $T > \Theta_D/2$ and, (3), is approximated by (4) [6]

$$-\frac{d\ln f}{dT} = \frac{3E^2}{kc^2}\left({\Theta_D}^2 M\right)^{-1}. \tag{4}$$

By plotting ln A(absorption area) against$T$, Θ_D can be obtained from the slope of a straight line.

Temperature dependence of δ can be expressed as (5) [7]

$$\frac{d\delta}{dT} = -\frac{3Ek}{2Mc^2}, \tag{5}$$

Θ_D', Θ_D estimated from temperature dependence of δ, is derived by combining (4) and (5), *i.e.*,

$${\Theta_D}' = -\frac{\sqrt{2E}}{k}\left[\frac{d\delta/dT}{d\ln(A/A_{77K})/dT}\right]^{1/2}. \tag{6}$$

In the case of ^{57}Fe, (6) is expressed as

$${\Theta_D}' = 4.327 \times 10^2\left[\frac{d\delta/dT}{d\ln[A/A_{77K}]/dT}\right]^{1/2} \tag{7}$$

Debye temperature was estimated by using the obtained δ and A values for each components, as listed in Table 2. By using (7), Θ_D' values of $280_{\pm 4.15}$ K for $Fe^{III}(T_d)$ and $307_{\pm 5.70}$ K for $Fe^{II+III}(O_h)$ were estimated for bulk Fe_3O_4, while smaller Θ_D's of $267_{\pm 5.45}$ and $282_{\pm 7.17}$ K were obtained for the corresponding components of NP $Fe_{3-x}O_4$. On the other hand, Mössbauer spectra of NP γFe_2O_3 composed of one sextet with δ, H_{int} and Γ of $0.40_{\pm 0.02}$ mm s^{-1}, $51.2_{\pm 0.14}$ T and $0.85_{\pm 0.11}$ mm s^{-1} at 77 K, and $0.33_{\pm 0.03}$ mm s^{-1}, $46.4_{\pm 0.27}$ T and $1.21_{\pm 0.11}$ mm s^{-1} at 300 K, respectively. Θ_D' of NP and bulk γFe_2O_3 was respectively calculated to be $259_{\pm 4.00}$ and $265_{\pm 1.05}$ K. These results show that NP $Fe_{3-x}O_4$ was oxidized to be NP γFe_2O_3 after annealing at 250 °C for 30 min, and that the chemical environment of iron in NPs of Fe_3O_4 and γFe_2O_3 is less rigid than that of bulk compounds. No significant differences in values of the Debye temperature (Θ_D) were estimated by using (4).

As shown in Fig. 3, XRD pattern of NP $Fe_{3-x}O_4$ showed peaks with broader linewidth observed at 2θ of 30.2°, 35.7°, 43.3°, 53.7°, 57.3° and 62.8° attributed to

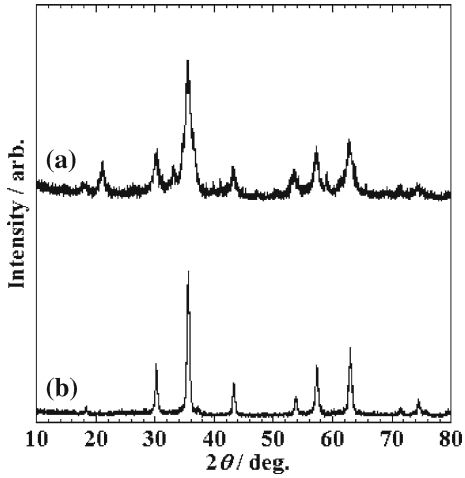

Fig. 3 XRD patterns of (**a**) $Fe_{3-x}O_4$ and (**b**) γ-Fe_2O_3 nanoparticles

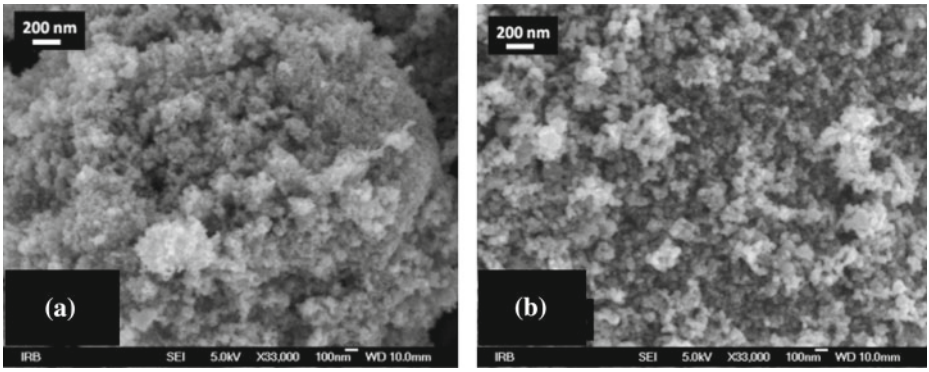

Fig. 4 FE-SEM images of (**a**) $Fe_{3-x}O_4$ and (**b**) γ-Fe_2O_3 nanoparticles

Fe_3O_4 (PDF No. 00-019-0629) and γFe_2O_3 (PDF No. 00-039-1346). It is difficult for distinguishing Fe_3O_4 and γFe_2O_3 because they both have identical inverse spinel structure and similar lattice parameters. A size of short-range order of NP $Fe_{3-x}O_4$ can be estimated by applying the Scherrer's formula [8, 9], *i.e.*,

$$t = K\lambda / B\, cos\Theta, \tag{8}$$

where t, K, λ, B and Θ are a size of short-range order (in nm), shape factor (= 0.849–1.107), wavelength of X-ray from Cu-K_α (= 0.1541 nm), FWHM and Θ at the peak (in radian), respectively. By using FWHM value of 0.44° obtained from (311) plane of the XRD pattern, the crystallite size of NP $Fe_{3-x}O_4$ was determined to be 29–37 nm. NP γFe_2O_3 prepared by annealing of NP $Fe_{3-x}O_4$ at 250 °C for 30 min did not show significant difference in the crystallite size. Consistent results were obtained from the FE-SEM observation of NPs of $Fe_{3-x}O_4$ and γFe_2O_3 having the particle size of 30–40 nm as shown in Fig. 4.

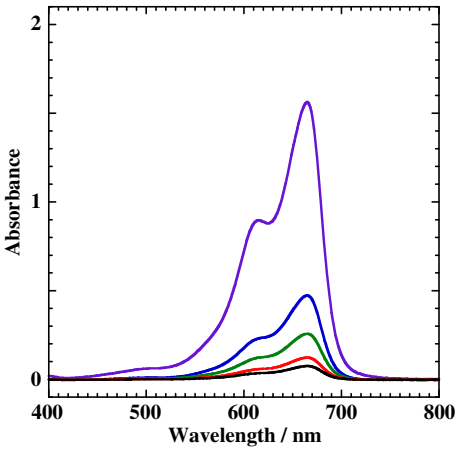

Fig. 5 UV-Vis spectra of bulk Fe^0-NP γFe_2O_3 mixture (3:7) measured after leaching test with 2.0×10^{-2} mM MB_{aq} for 0 (*purple*), 6 (*blue*), 12 (*green*), 18 (*red*) and 24 (*black*) hour

UV-Vis spectra of 2.0×10^{-2} mM methylene blue (MB) aqueous solution before and after 24-hour leaching with a mixture of bulk Fe^0-NP γFe_2O_3(3:7) are shown in Fig. 5. MB concentration was calculated by the Beer-Labert equation, *i.e.*,

$$Abs. = \varepsilon C_t l, \tag{9}$$

where *Abs.*, ε, C_t and l are absorbance, molar absorption coefficient ($= 7.9 \times 10^5$ $Lmol^{-1}$ cm^{-1} at 660 nm for MB [10]), concentration of MB solution after t-min leaching and optical path length (1 cm), respectively. Decrease in MB concentration was observed from 1.92×10^{-2} to 5.99×10^{-3}, 3.24×10^{-3}, 1.16×10^{-3} and 9.49×10^{-4} mol L^{-1} after leaching of 0, 6, 12, 18 and 24 h, respectively. A rate constant of first order reaction for MB decomposition(k_{MB}) can be estimated by (10),

$$C_t = C_0 \exp(-k_{MB} t)\,. \tag{10}$$

As a result of $\ln(C_t/C_0)$ *vs.* t plot, k_{MB} was determined to be 2.1×10^{-3} min^{-1}. Our previous study revealed that MB was decomposed by Fe^0-γFe_2O_3 '*bulk*' mixture (3:7) with the smaller k_{MB} of 1.6×10^{-1} day^{-1} ($= 1.1 \times 10^{-4}$ min^{-1}) [11]. These results prove that MB decomposing ability of Fe^0-γFe_2O_3 mixture (3:7) was increased when the NP γFe_2O_3 was utilized. It is concluded that environmental purifying ability will be improved by using nanoparticles of iron oxides.

4 Summary

NPs of $Fe_{3-x}O_4$ were prepared by hydrothermal reaction and the structure was characterized by ^{57}Fe-Mössbauer spectroscopy and XRD. Chemical reaction of $(NH_4)_2Fe(SO_4)\cdot 6H_2O$ and $FeCl_3\cdot 6H_2O$ using an autoclave provided defective $Fe_{3-x}O_4$ with 'x' of 0.124 having the particle size of 29–37 nm. Mössbauer spectra of NP $Fe_{3-x}O_4$ are composed of two relaxed sextets with δ, H_{int}, Γ and A of $0.34_{\pm 0.03}$ mm s^{-1}, $49.0_{\pm 0.30}$ T, $1.09_{\pm 0.03}$ mm s^{-1} and 56.3 % for tetrahedral Fe^{III}, and $0.66_{\pm 0.11}$ mm s^{-1}, $44.0_{\pm 0.71}$ T, $1.55_{\pm 0.31}$ mm s^{-1} and 43.7 % for octahedral (O_h) Fe^{II+III}, respectively. On the other hand, the Mössbauer spectrum of NP γFe_2O_3 prepared from annealing of NP $Fe_{3-x}O_4$ at 250 °C for 30 min consisted of one sextet with δ, H_{int} and Γ of

$0.33_{\pm 0.03}$ mm s^{-1}, $46.4_{\pm 0.27}$ T and $1.21_{\pm 0.11}$ mm s^{-1}, respectively. Debye temperature (Θ_D') of each component of NP $Fe_{3-x}O_4$ was respectively estimated to be $267_{\pm 5.45}$ K for Fe^{III}(T_d) and $282_{\pm 7.17}$ K for Fe^{II+III}(O_h), both of which were smaller than that obtained for bulk Fe_3O_4 of $280_{\pm 4.15}$ K and $307_{\pm 5.70}$ K. A smaller Θ_D' of $259_{\pm 4.00}$ K was also obtained for NP γFe_2O_3. These results indicate that the chemical environment of iron in nano particles is less rigid than that of bulk materials. Methylene blue (MB) decomposing rate caused by bulk Fe^0-NP γFe_2O_3mixture was calculated to be 2.1×10^{-3} min^{-1}, indicating that MB was effectively decomposed by using nanoparticle. It is concluded that NP $Fe_{3-x}O_4$is one of the effective materials for environmental purification.

References

1. Liang, X., Zhong, Y., Zhu, S., Ma, L., Yuan, P., Zhu, J., He, H., Jiang, Z.: The contribution of vanadium and titanium on improving methylene blue decolorization through heterogeneous UV-Fenton reaction catalyzed by their co-doped magnetite. J. Hazard. Mater. **199–200**, 247–254 (2012)
2. Pathak, T.K., Vasoya, N.H., Natarajan, T.S., Mobi, K.B., Tayabe, R.J.: Photocatalytic degradation of aqueous nitrobenzene solution using nanocrystalline Mg-Mn ferrites. Mater. Sci. Forum **764**, 116–129 (2013)
3. Kubuki, S., Shibano, K., Akiyama, K., Homonnay, Z., Kuzmann, E., Ristić, M., Nishida, T.: Effect of the structural change of an iron-iron oxide mixture on the decomposition of trichloroethylene. J. Radioanal. Nucl. Chem. **295**, 23–30 (2012)
4. Topsøe, H., Dumesic, J.A., Boudart, M.: Mössbauer spectra of stoichimetric and non stoichiometric Fe_3O_4 microcrystals. J. Phys., Colloque C6. **35**(supplément au n° 12), C6–411 (1974)
5. Homonnay, Z., Musić, S., Nishida, T., Kopelev, N.S., Vertés, A.: ch.1 Physical basis of Mössbauer spectroscopy. In: Vértes, A., Homonnay, Z. (eds.) Mössbauer Spectroscopy of Sophisticated Oxides, pp. 1–26, Akademiai Kiado, Budapest (1997)
6. Nishida, T.: Advances in the Mössbauer effect for the structural study of glasses. J. Non-Cryst. Solids **177**, 257–268 (1994)
7. Katada, M., Herber, R.: Lattice dynamics and hyperfine interactions of intercalation compounds $FexTiS_2$ (x = 1/4, 1/3 and 1/2) and $Fe_{1/3}NbS_2$ from ^{57}Fe Mössbauer spectroscopy. J. Solid State Chem. **33**(3), 361–369 (1980)
8. Scherrer, P.: Bestimmung der Größe und der inneren Struktur von Kolloidteilchen mittels Röntgenstrahlen. Göttinger Nachrichten Gesell. **2**, 98–100 (1918)
9. Patterson, A.: The Scherrer formula for X-ray particle size determination. Phys. Rev. **56**(10), 978–982 (1939)
10. Wakasa, M.: Magnetic field effects on the photocatalytic reaction. Research Report of Comprehensive Research Organization, vol. 4. http://sucra.saitama-u.ac.jp/modules/xoonips/download.php/KP17A05-76.pdf?file_id=1427 (in Japanese) (2006)
11. Kubuki, S., Shibano, K., Akiyama, K., Homonnay, Z., Kuzmann, E., Ristić, M., Nishida, T.: Decomposition mechanism of methylene blue caused by metallic iron-maghemite mixture. Hyperfine Interact. **218**, 47–52 (2013)